

# Quantitative DFT modeling of enantiomeric excess for dioxirane-catalyzed epoxidations.

## Supporting information 1.

Severin T. Schneebeli, Michelle Lynn Hall, Ronald Breslow\*, Richard Friesner\*

Department of Chemistry, Columbia University, New York, New York, 10027

rb33@columbia.edu, rich@chem.columbia.edu

**Table S1.** M06-2X/6-31G\*(solution) and B3LYP/6-311+G\*\*\*(solution)//B3LYP/6-31G\*(solution) results.

Entry	Catalyst	Olefin	Exp. <sup>3</sup>	$\Delta G^{\text{TS}}$ (kcal/mol) (% ee)				Ref. <sup>1</sup>	Solv. <sup>2</sup>
				M06-2X <sup>4</sup>	larger basis <sup>5</sup>				
1	1	e	0.22 (18)	-1.37 (-65)	-0.17 (-9.4)			I	A
2	1	b	0.75 (56)	0.97 (50)	0.23 (13.0)			I	A
3	1	c	1.18 (76)	1.02 (52)	1.01 (51.5)			I	A
4	1	f	1.10 (73)	-1.91 (-79)	-0.18 (-10.1)			I	A
5	1	d	1.00 (69)	0.70 (37)	1.15 (57.0)			I	A
6	1	g	0.26 (22)	0.60 (32)	0.15 (8.6)			I	A

<sup>1</sup> Experimental references: (I) Armstrong, A.; Ahmed, G.; Dominguez-Fernandez, B.; Hayter, B. R.; Wailes, J. S. *J. Org. Chem.* **2002**, *67*, 8610.. (II) Solladié-Cavallo, A.; Jierry, L.; Klein, A.; Schmitt, M.; Welter, R. *Tetrahedron: Asymmetry* **2004**, *15*, 3891. (III) Denmark, S. E.; Matsuhashi, H. *J. Org. Chem.* **2002**, *67*, 3479. (IV) Armstrong, A.; Dominguez-Fernandez, B.; Tsuchiya, T. *Tetrahedron* **2006**, *62*, 6614. (V) Armstrong, A.; Moss, W. O.; Reeves, J. R. *Tetrahedron: Asymmetry* **2001**, *12*, 2779. (VI) Armstrong, A.; Tsuchiya, T. *Tetrahedron* **2005**, *62*, 257. (VII) Wang, Z.; Shi, Y. *J. Org. Chem.* **2001**, *66*, 521. (VIII) Burke, C. P.; Shi, Y. *Angew. Chem. Int. Ed.* **2006**, *45*, 4475.

<sup>2</sup> Solvent systems: (A) 3:2 CH<sub>3</sub>CN:H<sub>2</sub>O (v:v), dielectric constant,  $\epsilon$ , employed in the continuum solvation model: 55 (B) 2:1 dioxane:H<sub>2</sub>O (v:v),  $\epsilon$  = 20 (C) 3:1 CH<sub>3</sub>CN:H<sub>2</sub>O (v:v),  $\epsilon$  = 47 (D) 3:3:6.4 DMM:CH<sub>3</sub>CN:H<sub>2</sub>O (v:v:v),  $\epsilon$  = 69 (E) 26:1:2.8 H<sub>2</sub>O:DMM:DME (v:v:v),  $\epsilon$  = 73.

<sup>3</sup> Experimental  $\Delta G^{\text{TS}}$ .

<sup>4</sup> Results at the M06-2X/6-31G\*(solution) level. Zero point energies were obtained from the B3LYP/6-31G\*(vacuum) frequency calculations. The ee values were obtained from scaled  $\Delta G^{\text{TS}}$ . (Scaling Factor = 2/3).

<sup>5</sup> Results at the B3LYP/6-311+G\*\*\*(solution)//B3LYP/6-31G\*(solution) level. The ee values were obtained from scaled  $\Delta G^{\text{TS}}$ . (Scaling Factor = 2/3).

Entry	Catalyst	Olefin	$\Delta G^{\text{TS}}$ (kcal/mol) (% ee)					Ref. <sup>1</sup>	Solv. <sup>2</sup>
			Exp. <sup>3</sup>	M06-2X <sup>4</sup>	larger basis <sup>5</sup>	Ref. <sup>1</sup>	Solv. <sup>2</sup>		
7	1	a	0.35 (29)	0.82 (43)	0.41 (22.7)	I	A		
8	1	h	1.41 (83)	3.28 (95.1)	0.94 (48.4)	I	A		
9	2	c	0.72 (54)	0.93 (48)	2.44 (87.9)	I	A		
10	3	c	1.53 (86)	-0.96 (-49)	1.38 (65)	I	A		
11	8	b	0.26 (22)	-0.09 (-5)	0.61 (33)	II	B		
12	9	b	0.00 (0)	0.37 (21)	-0.24 (-13)	II	B		
13	7	b	1.03 (70)	1.95 (80)	0.93 (48)	II	B		
14	7	c	1.53 (86)	2.26 (86)	1.77 (76)	II	B		
15	10	b	1.49 (88)	5.01 (99.6)	1.20 (63)	III	A		
16	10	c	1.89 (94)	6.14 (99.9)	3.08 (96)	III	C		
17	10	d	0.74 (59)	5.01 (99.6)	1.10 (59)	III	A		
18	10	i	0.50 (43)	3.85 (98.3)	-0.04 (-3)	III	A		
19	4	c	1.41 (83)	0.82 (43)	1.69 (74)	IV	A		
20	6	c	0.90 (64)	8.68 (99.9)	1.26 (61)	IV	A		
21	6	a	0.02 (2)	0.73 (39)	0.26 (15)	IV	A		
22	5	a	0.62 (48)	0.67 (36)	0.39 (22)	V	A		
23	5	c	1.96 (93)	-1.30 (-63)	1.69 (74)	V	A		
24	5	d	1.37 (82)	-1.47 (-68)	0.86 (45)	V	A		
25	5	h	2.72 (98)	2.16 (84)	1.86 (78)	V	A		
26	5	j	0.04 (3)	-0.68 (-36)	0.78 (41)	V	A		
27	11	g	0.08 (7)	na (na)	-0.59 (-32)	VI	A		
28	11	a	0.23 (19)	na (na)	-0.55 (-30)	VI	A		
29	14	c	2.27 (97)	6.49 (99.9)	4.98 (99.6)	VII	D		
30	15	c	1.49 (88)	4.41 (99.1)	2.23 (88)	VII	D		
31	16	c	1.54 (89)	na (na)	1.65 (77)	VII	D		
32	18	c	0.86 (66)	1.54 (74)	2.38 (90)	VII	D		
33	19	c	0.98 (72)	2.23 (87.9)	2.78 (93.6)	VII	D		
34	14	a	0.16 (15)	0.87 (50)	-1.59 (-77)	VII	D		
35	15	a	0.16 (15)	-0.63 (-38)	0.21 (13)	VII	D		
36	16	a	0.34 (31)	na (na)	0.41 (26)	VII	D		
37	17	a	0.26 (24)	na (na)	0.29 (18)	VII	D		
38	18	a	0.15 (14)	0.87 (50)	0.13 (8)	VII	D		
39	14	b	1.66 (92)	2.63 (93.3)	0.74 (44)	VII	D		
40	15	b	1.39 (87)	3.27 (97.0)	-0.15 (-9)	VII	D		
41	16	b	1.44 (88)	na (na)	4.57 (99.4)	VII	D		
42	17	b	1.07 (77)	6.30 (99.9)	-1.99 (-85)	VII	D		
43	18	b	0.52 (46)	1.93 (84)	0.43 (27)	VII	D		
44	19	b	0.42 (38)	1.40 (71)	0.68 (41)	VII	D		
45	13	k	1.66 (92)	na (na)	2.84 (94.8)	VIII	E		
46	12	l	1.73 (93)	na (na)	0.45 (28)	VIII	E		

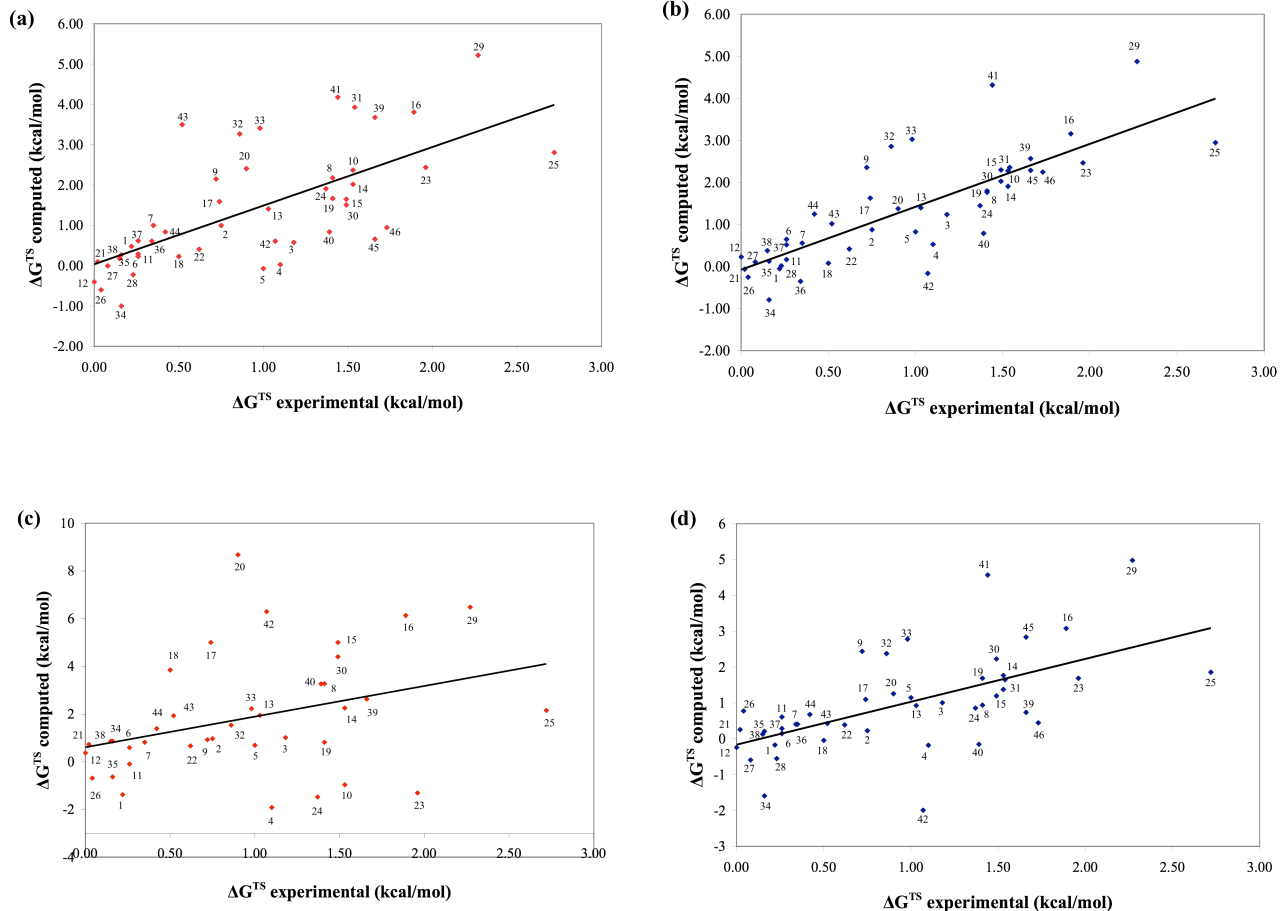


**Figure S1:** Experimental versus computed enantiomeric transition state energy differences,  $\Delta G^{TS}$ , for all reactions in the test set. Experimental versus computed enantiomeric transition state energy differences,  $\Delta G^{TS}$ , for all reactions in the test set. (a) B3LYP/6-31G\*(solution)// B3LYP/6-31G\*(vacuum) level. (Solid line shows linear least squares fit of  $y = 1.45x + 0.04$  with coefficient of determination  $R^2 = 0.46$ ) (b) B3LYP/6-31G\*(solution) level ( $y = 1.49x - 0.07$ ,  $R^2 = 0.64$ ). (c) M06-2X/6-31G\*(solution) level. (Solid line shows linear least squares fit of  $y = 1.29x + 0.61$  with coefficient of determination  $R^2 = 0.12$ ) (d) B3LYP/6-311+G\*\*\*(solution)//B3LYP/6-31G\*(solution) level ( $y = 1.19x - 0.16$ ,  $R^2 = 0.36$ ). All data points are labeled with the corresponding reaction numbers.

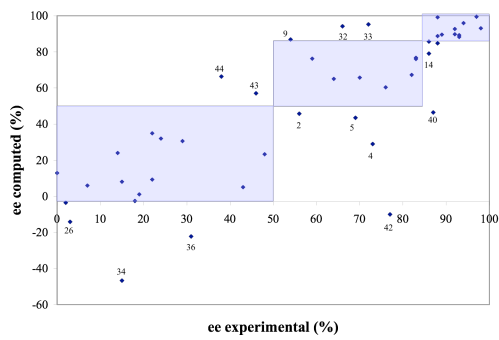


**Figure 3:** Experimental versus computed % ee for solution phase transition states at the B3LYP/6-31G\*(solution) level. Shaded areas represent regions where computed and experiment fall within the same category of percent enantiomeric excess, i.e. low (0-50), medium (50-85) and high (85-100). Reactions that do not fall into the correct region are labeled with their corresponding reaction numbers.

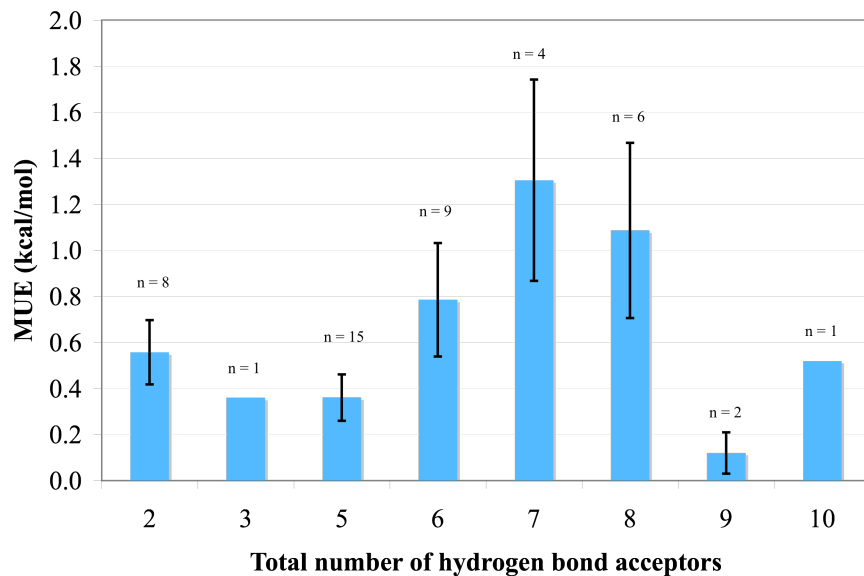


**Figure S2:** Mean unsigned error (MUE) as a function of the total number of hydrogen bond acceptors present in the transition states. Only Oxygen and Nitrogen were counted as hydrogen bond acceptors. n = sample size. Error bars represent standard error. No error bars are shown for n = 1.

**Table S2.** Boltzman weighted forming bond distances (O3-C4 and O3-C5 in Figure 1) in Å of the transition states at the B3LYP/6-31G\*(solution)//B3LYP/6-31G\*(vacuum) and the B3LYP/6-31G\*(solution) level.

Reaction #	vacuum structures		solution phase structures	
	shorter	longer	shorter	longer
1	2.03	2.37	2.22	2.48
2	1.97	2.33	2.16	2.44
3	1.99	2.24	2.20	2.31
4	2.00	2.29	2.19	2.38
5	2.02	2.38	2.21	2.48
6	1.98	2.46	2.17	2.59
7	1.96	2.39	2.14	2.50
8	2.00	2.39	2.11	2.42
9	2.01	2.11	2.21	2.22
10	1.95	2.20	2.12	2.29
11	1.90	2.27	2.06	2.35
12	1.93	2.25	2.12	2.37
13	1.96	2.33	2.14	2.43
14	1.96	2.23	2.14	2.30
15	1.98	2.30	2.24	2.41
16	2.01	2.12	2.25	2.29
17	2.02	2.34	2.24	2.53
18	1.93	2.37	2.13	2.47
19	1.99	2.19	2.20	2.31
20	2.03	2.26	2.18	2.42
21	2.02	2.42	2.19	2.56
22	1.90	2.36	2.08	2.48
23	2.00	2.08	2.16	2.22
24	1.97	2.33	2.14	2.47
25	1.97	2.46	2.12	2.55
26	1.89	2.15	2.05	2.11
27	1.94	2.42	2.17	2.58
28	1.94	2.36	2.14	2.52
29	2.00	2.11	2.11	2.13
30	1.94	2.21	2.00	2.23
31	1.99	2.12	2.12	2.21
32	2.01	2.21	2.23	2.34
33	2.02	2.21	2.22	2.25
34	1.94	2.38	2.14	2.52
35	1.93	2.39	2.11	2.51
36	1.94	2.40	2.12	2.53
37	1.93	2.37	2.14	2.51
38	1.97	2.36	2.16	2.48
39	1.99	2.27	2.22	2.44
40	1.93	2.29	2.13	2.37
41	1.95	2.38	2.14	2.46

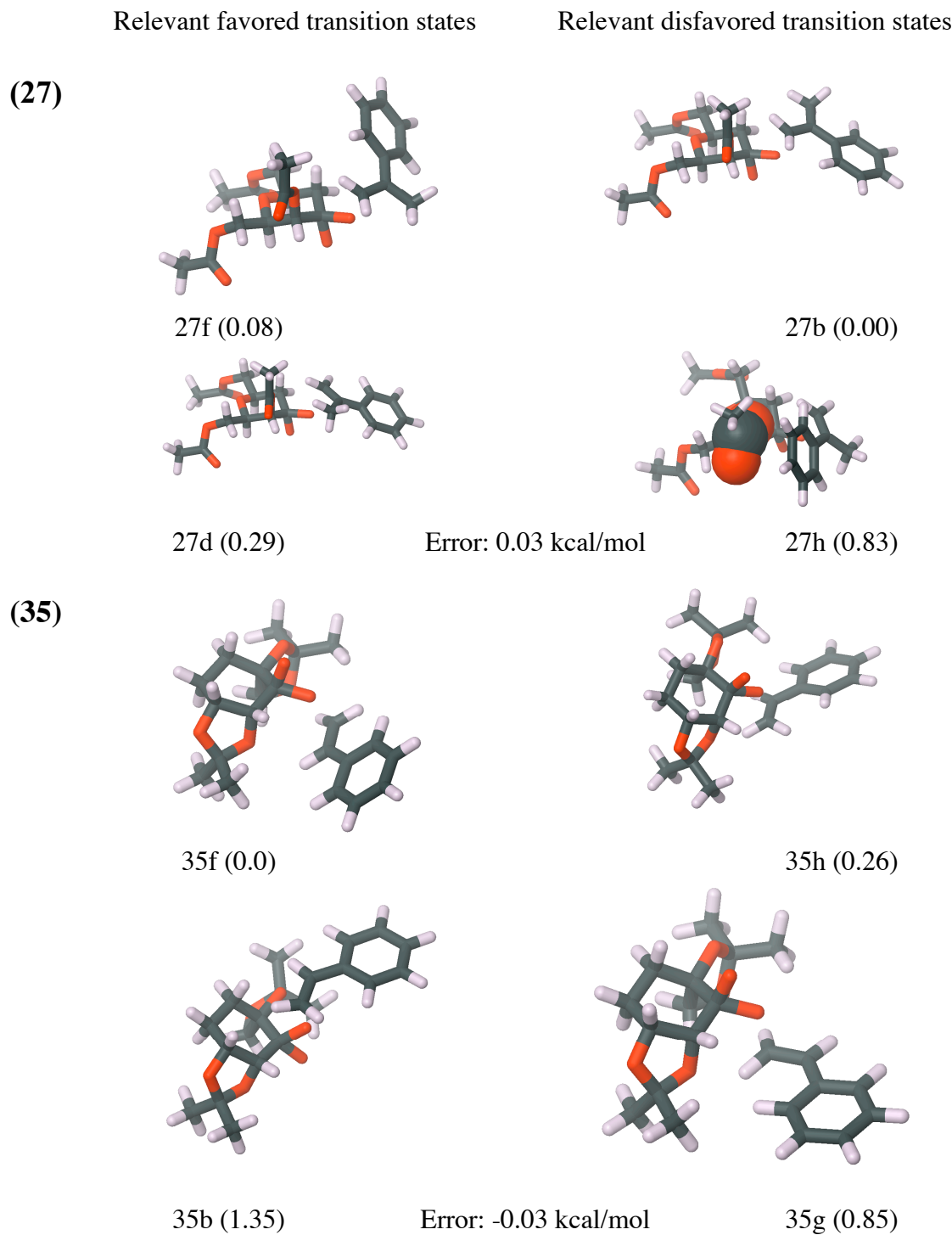
Reaction #	vacuum structures		solution phase structures	
	shorter	longer	shorter	longer
42	1.94	2.33	2.05	2.30
43	1.91	2.30	2.21	2.43
44	2.00	2.35	2.19	2.42
45	1.94	2.38	1.92	2.37
46	1.97	2.22	2.19	2.53

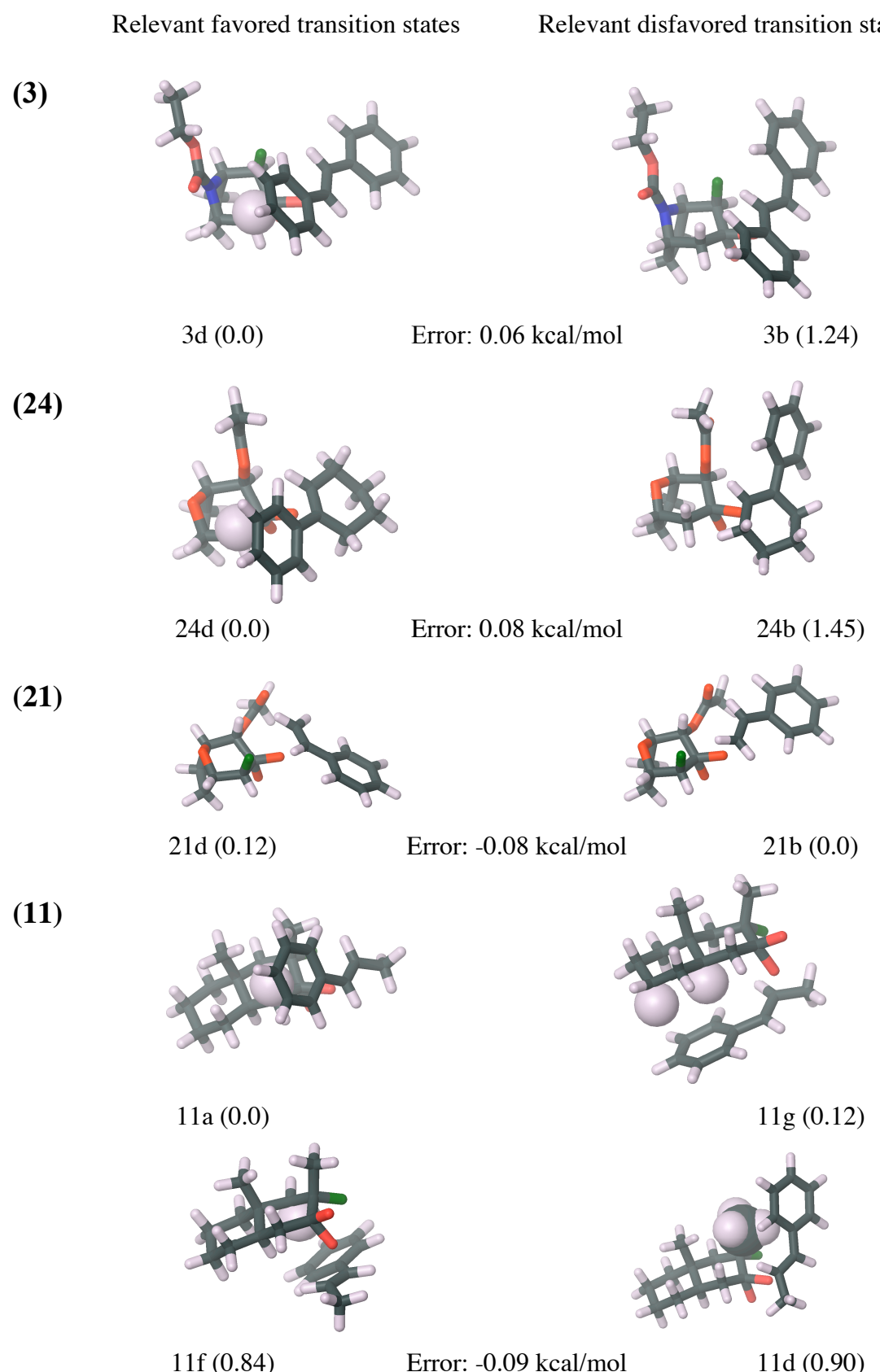
**Table S3.** Boltzman-weighted dihedral angles  $\theta$  (shown in Figure 8) at the B3LYP/6-31G\*(solution) level for each ensemble of favored and disfavored transition states.

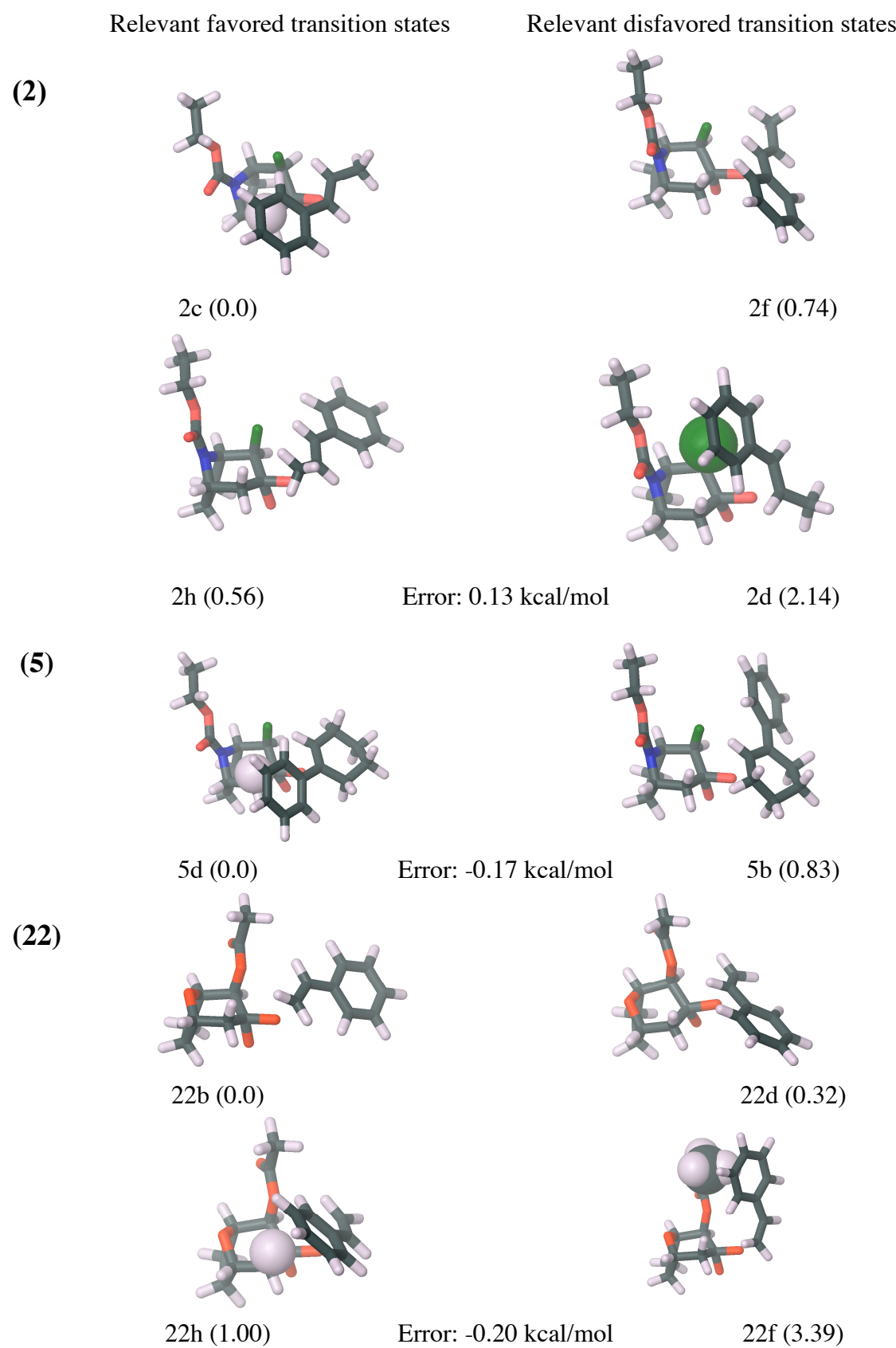
Reaction #	$\theta$ (Degrees)	
	Favored	Disfavored
1	91.0	116.3
2	96.8	133.6
3	91.9	123.3
4	97.1	128.6
5	110.5	128.0
6	123.4	110.4
7	95.0	98.1
8	102.0	123.7
9	99.0	120.7
10	91.4	136.2
11	99.3	98.3
12	98.9	95.4
13	98.9	128.4
14	98.1	135.6
15	94.3	132.9
16	93.3	100.3
17	97.2	133.4
18	96.8	103.9
19	92.2	120.6
20	105.1	118.7
21	106.1	95.2
22	105.9	112.3
23	96.4	141.8
24	90.1	140.4
25	92.1	141.5
26	111.9	103.3
27	123.3	136.2
28	92.9	108.7
29	94.2	114.6
30	95.1	92.2
31	102.6	118.2
32	90.6	92.3
33	92.0	95.5
34	98.7	117.8
35	100.6	126.0
36	126.9	116.6
37	101.9	115.4
38	92.9	103.3
39	98.3	133.2
40	90.3	106.8
41	95.1	106.1

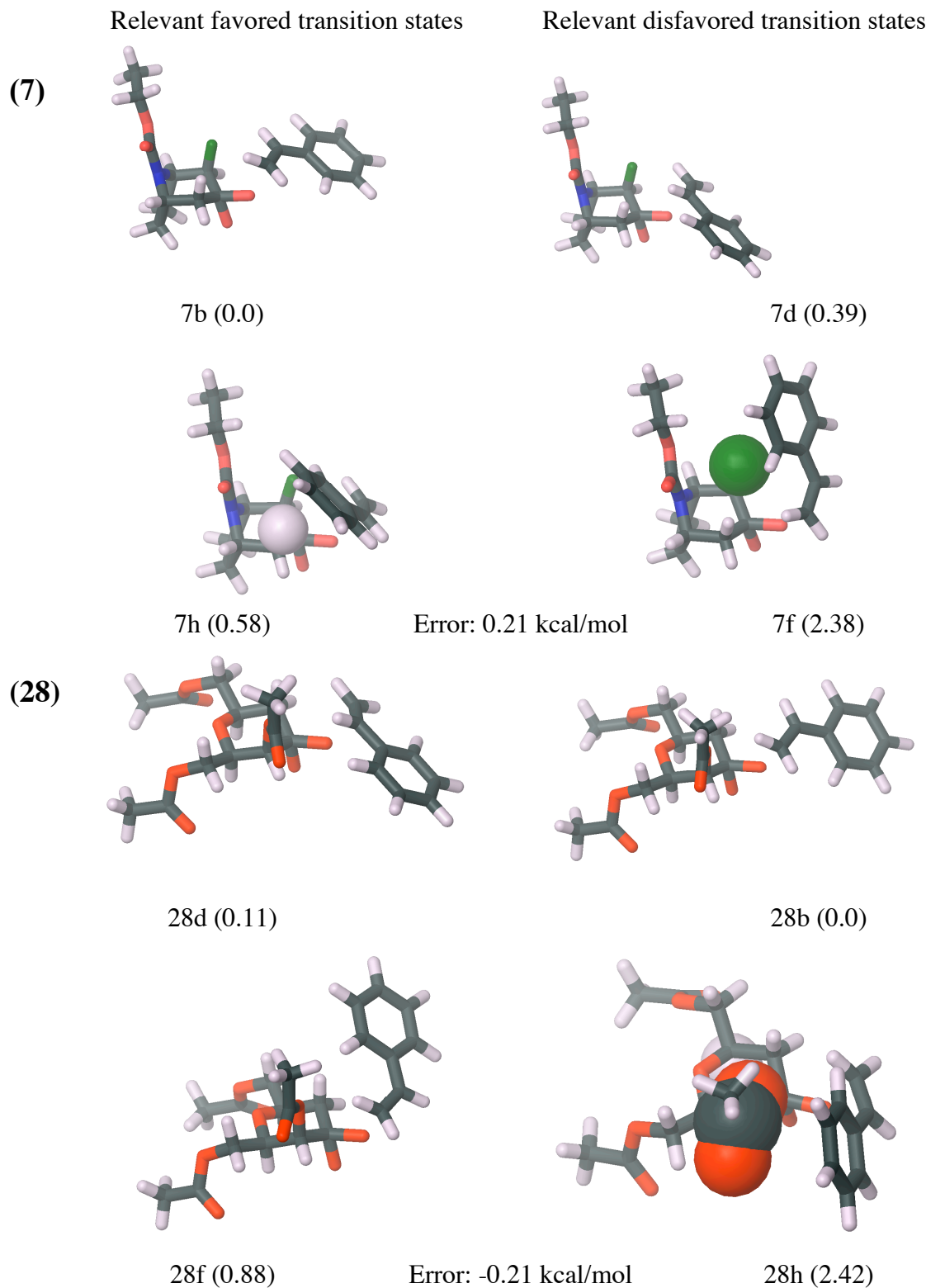
Reaction #	$\theta$ (Degrees)	
	Favored	Disfavored
42	92.5	115.0
43	94.2	133.3
44	93.8	133.0
45	132.4	97.6
46	101.6	97.3

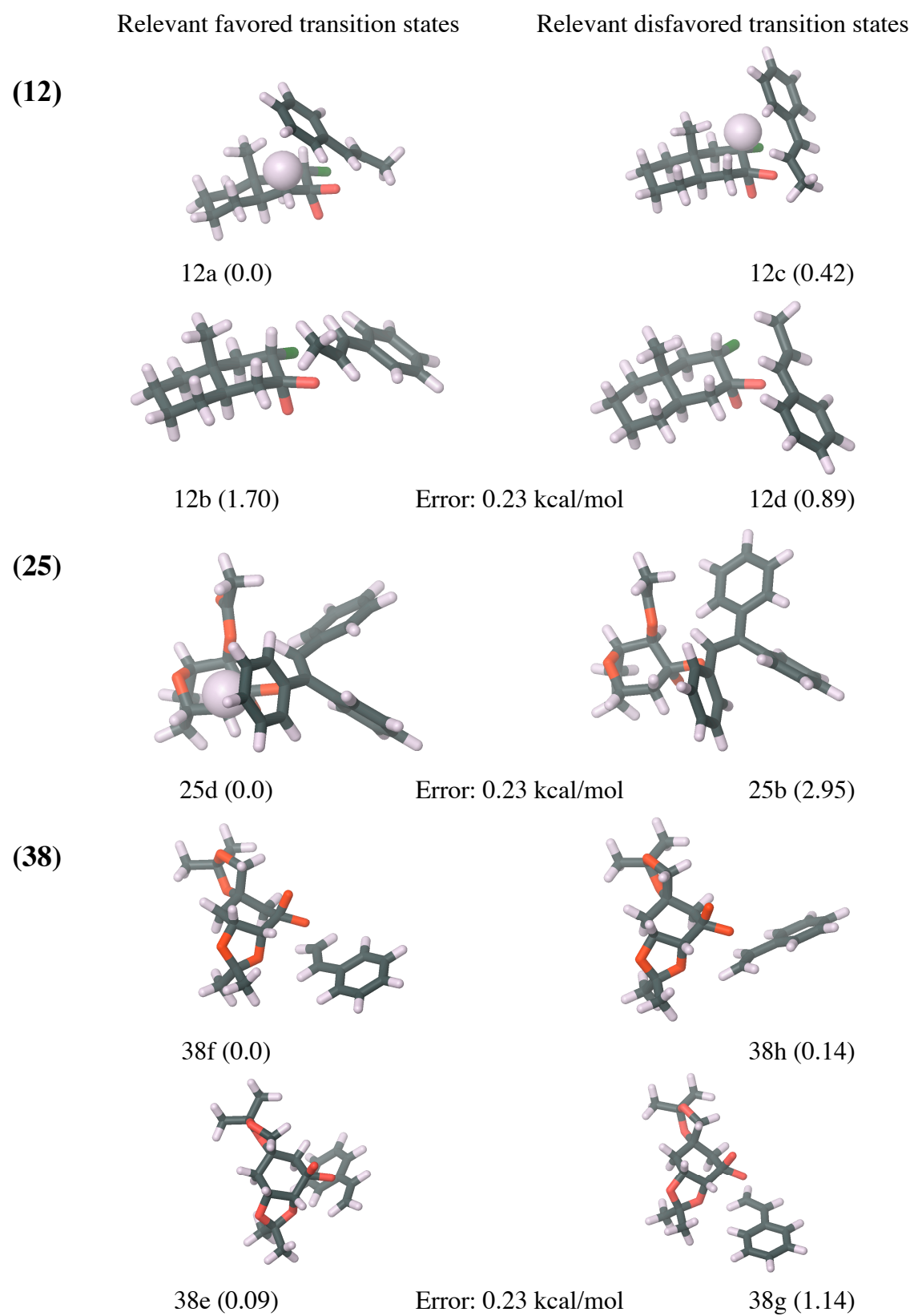
**Figure S4:** (pages 9 – 23). The relevant low energy favored and disfavored transition states at the B3LYP/6-31G\*(solution) level for all cases not shown in the main paper (ordered according to increasing absolute error). Deviations at the B3LYP/6-31G\*(solution) level from the experimental transition state free energy differences,  $\Delta G^{\text{TS}}$ , are given for each reaction. Relative energies of the transition states (B3LYP/6-31G\*(solution) level) (kcal/mol) are shown in brackets. Regions interacting mainly through dispersion interactions, for which B3LYP is assumed to be too repulsive, are shown in spacefilling mode. Atom colors: carbon (black), oxygen (red), hydrogen (white), nitrogen (blue), fluorine (green), chlorine (pink) and silicon (yellow).

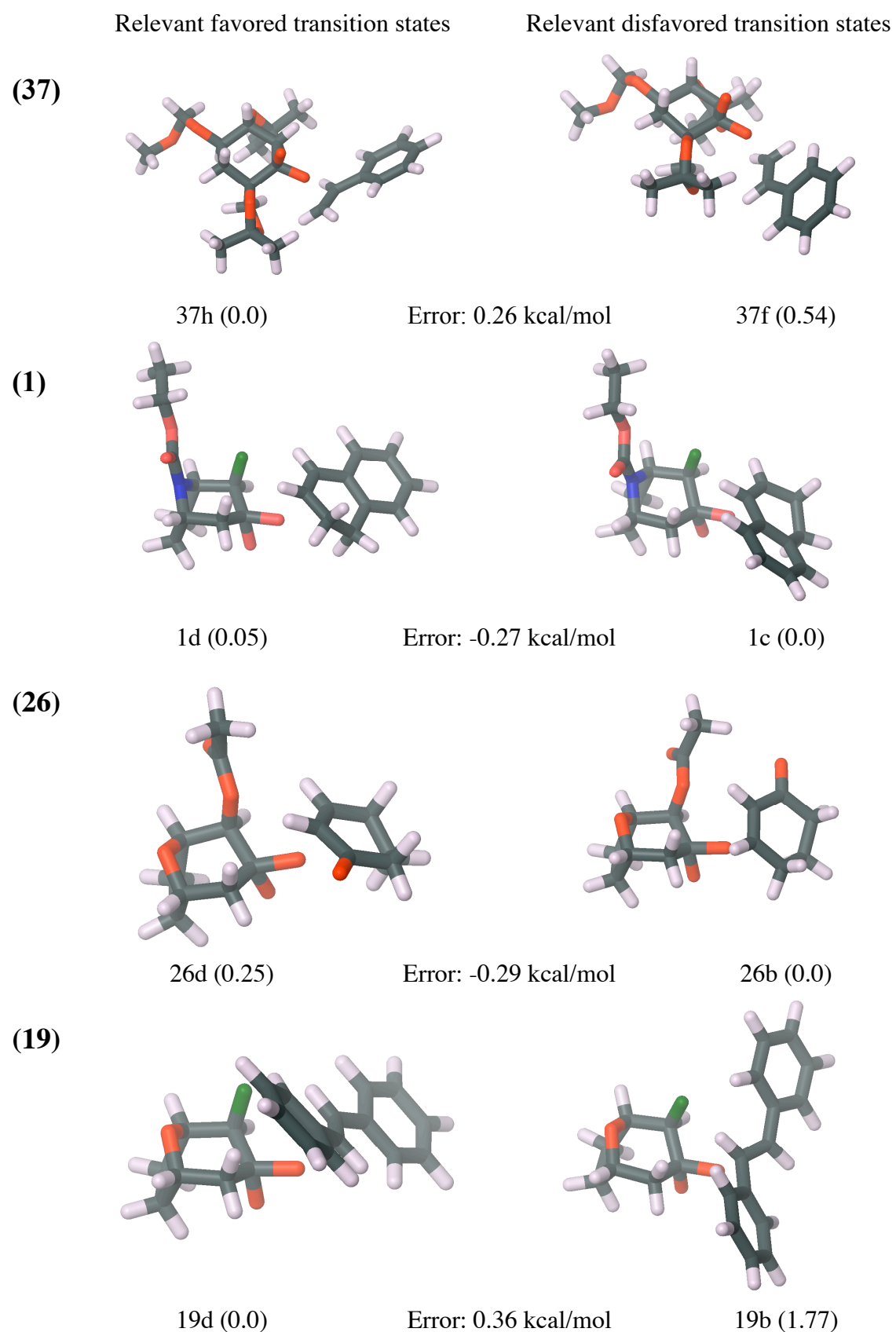


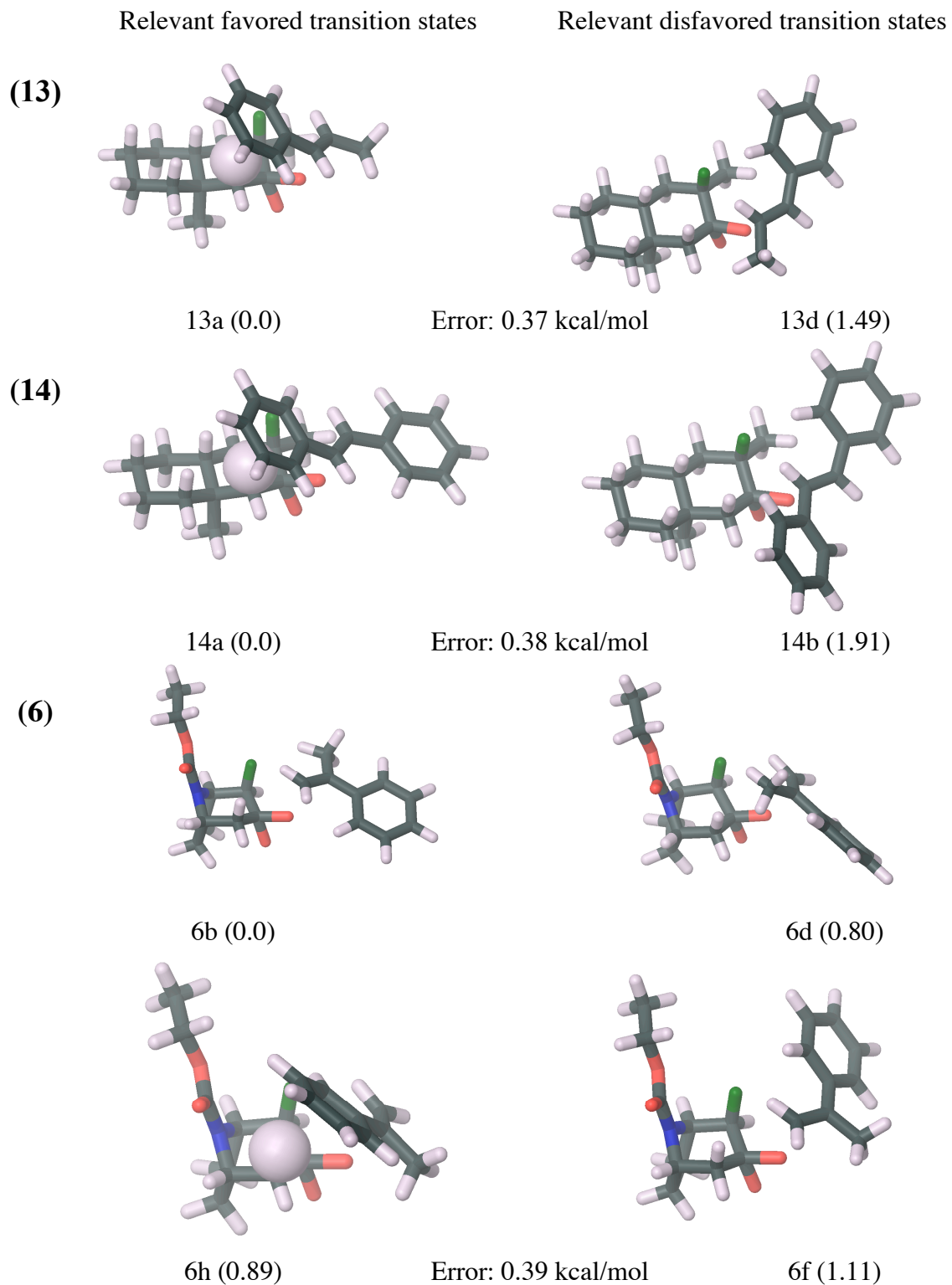


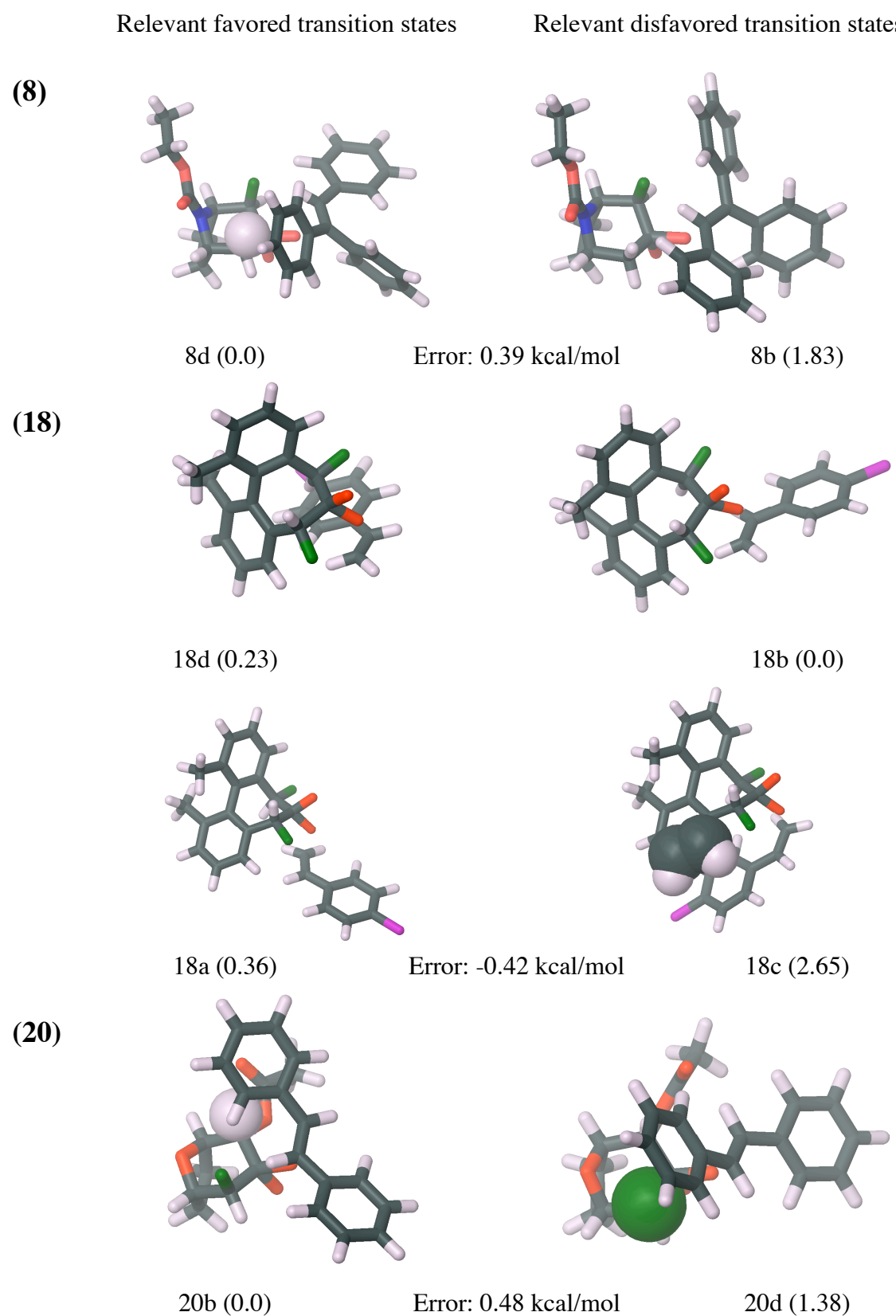


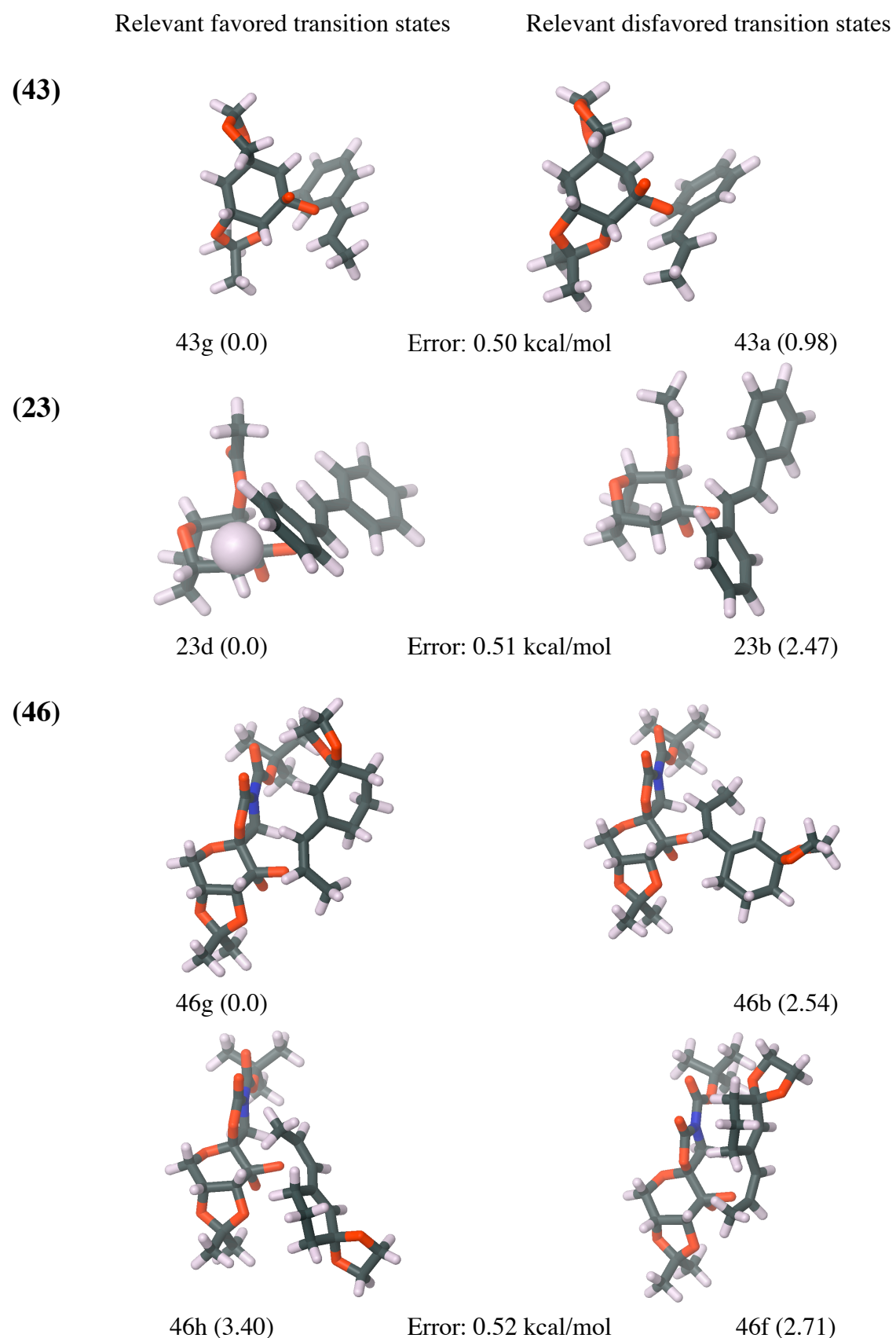


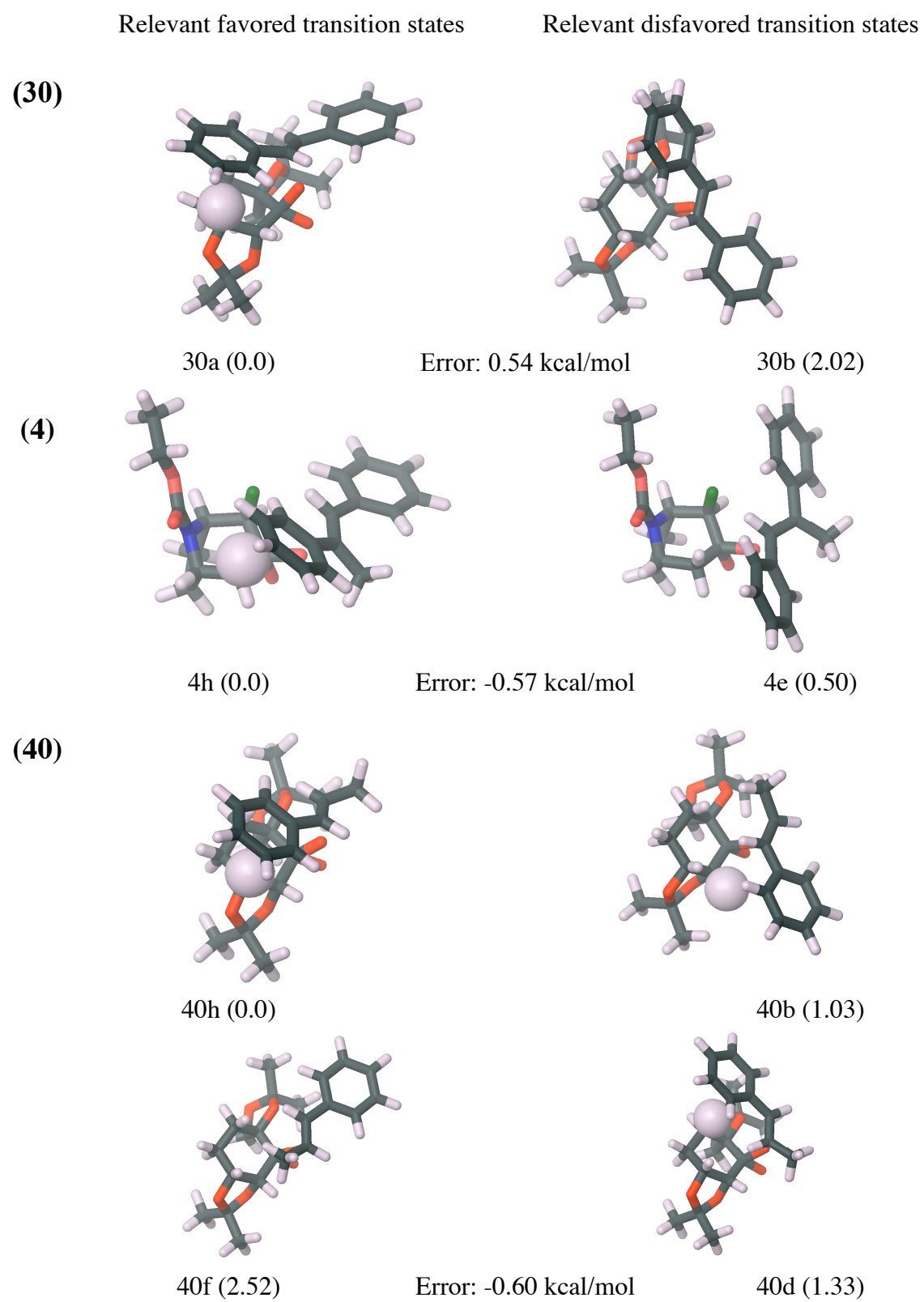


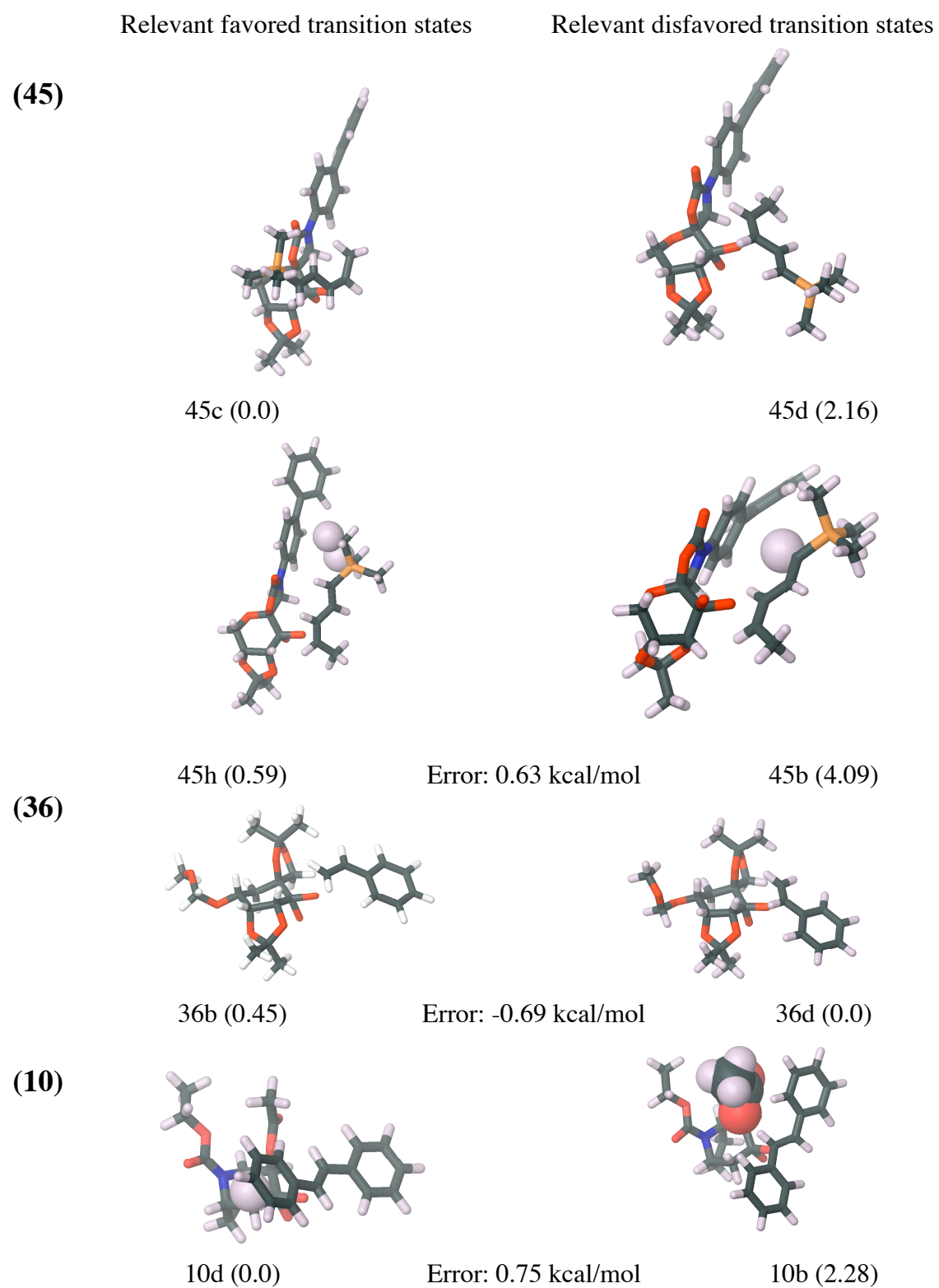


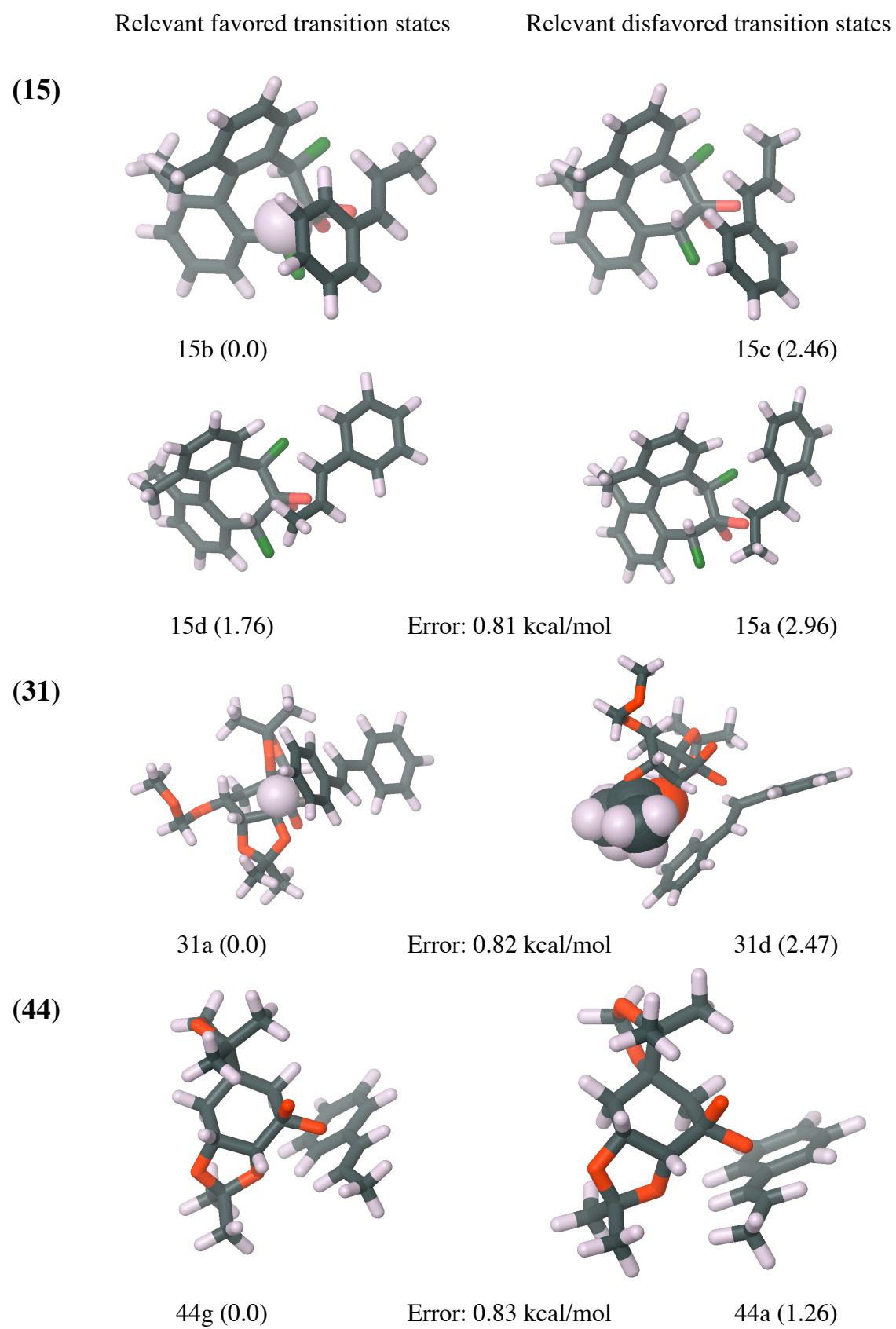






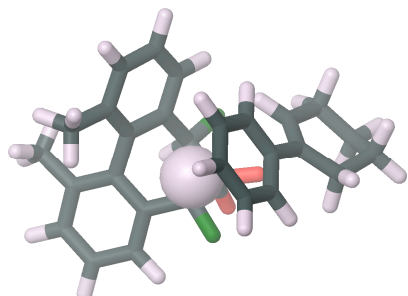






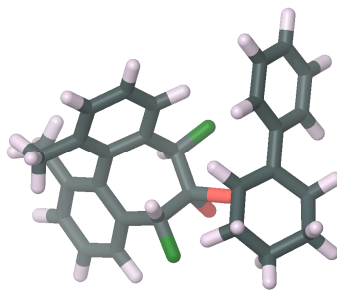
Relevant favored transition states

(17)



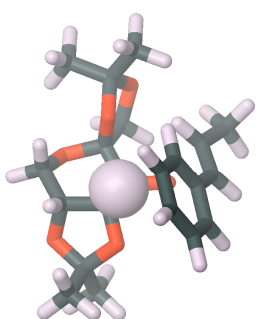
17b (0.0)

Relevant disfavored transition states

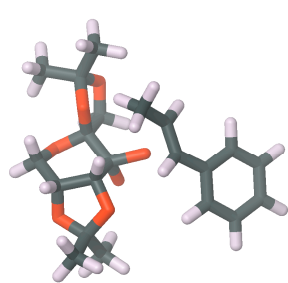


17a (1.63)

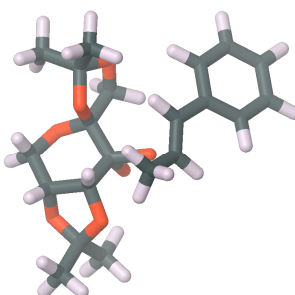
(39)



39a (0.0)

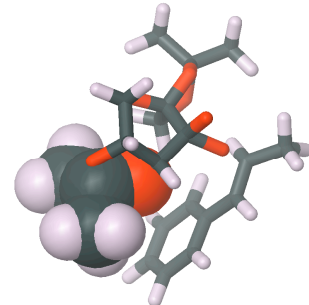


39f (2.60)



39b (0.86)

Error: 0.91 kcal/mol



39g (3.42)

